Population of higher-energy levels in $LiY_{1-x}Er_xF_4$ (x=0.003 ÷1) crystals under CW IR laser-diode pumping

A. M. Tkachuk[1], I. K. Razumova[1], A. A. Mirzaeva[2], G. E. Novikov[2], O. A. Orlov[2], A. V. Malyshev[3], and V. P. Gapontsev[4]

[1] Federal Research Center "Vavilov State Optical Institute", St. Petersburg, 199034 Russian Federation
[2] Institute for Laser Physics, St. Petersburg, 199034 Russian Federation
[3] A. I. Ioffe Physical-Technical Institute, St. Petersburg, 194121 Russian Federation,
[4]IPG-Laser, GmbH, Siemensstrasse, 7, D-57299 Burbach, Germany

ABSTRACT

Steady-state population of 7 lowest excited erbium levels in $LiY_{1-x}Er_xF_4$ (YLF:Er^{3+}) (x=0.003-1) crystals was studied under upconversion CW InGaAs laser-diode pumping with varied power density. Theoretical and experimental concentration and power dependencies of population of higher-energy radiative levels were obtained. Relative changes in populations of studied levels in YLF:Er^{3+} crystals were experimentally controlled by visible spectra of steady-state luminescence in the wavelength ranges corresponding to transitions $^4S_{3/2} \rightarrow {}^4I_{15/2}$ (0.52--0.57) μm and $^4F_{9/2} \rightarrow {}^4I_{15/2}$ (0.64--0.68) μm. IR-pumped luminescence kinetic curves of higher-energy transitions $^4S_{3/2} \rightarrow {}^4I_{15/2}$ (0.55 μm) and $^2H_{9/2} \rightarrow {}^4I_{15/2}$ (0.41 μm) were recorded. The energy-transfer mechanisms were determined, and the predominant mechanisms responsible for upconversion excitation were elucidated. Microparameters of energy transfer and concentration dependencies of the selfquenching rates and non-linear coupling were obtained on the basis of theoretical and experimental estimates of the rates of intra- and intercenter relaxation processes (migration, selfquenching, and upconversion) allowing for statistics of coupling between the impurity centers in the system. The steady-state dependencies of population on the erbium concentration and pumping power density were calculated within the framework of rate balance equations. Good agreement between the theory and experimental data was obtained.

Keywords: solid-state lasers, energy transfer, upconversion, laser-diode pumping

1. INTRODUCTION

Crystals doped with rare-earth ions in high concentrations are well-known active media with high gain coefficient promising for development of miniature lasers for different practical applications. Recently, it was a great interest to laser-diode pumped compact solid-state lasers emitting in a wide spectral range from IR to VIS. Possibility for a considerable increase in laser efficiency under upconversion pumping has been demonstrated.

Possibility for obtaining the inverse population of working levels of laser transitions strongly depends on macrorates of the interionic coupling processes since these processes define the working levels' population. Effect of the interionic coupling sharply increases with dopant concentration.

This work continues series of recent studies[1-4] of YLF: Er crystals upon IR LD cw pumping aimed at analytical description of the system involving excited states emitting in the IR and VIS spectral ranges. In our previous works we reported studies on the population of the levels emitting in the 3 μm, red, and green spectral regions. Present study considers also the upconversion processes between the exited levels including high-energy $^2G_{9/2}$ ($^2H_{9/2}$) and $^4G_{11/2}$ erbium levels.

Correspondence: A.M. Tkachuk. Email: tkachuk@mail.rcom.ru. Other author information:
V.P.G. E-mail: valentingapontsev@compuserve.com

XI Feofilov Symposium on Spectroscopy of Crystals Activated by Rare-Earth and Transition Metal Ions, Alexander A. Kaplyanskii, Boris Z. Malkin, Sergey I. Nikitin, Editors,
Proceedings of SPIE Vol. 4766 (2002) © 2002 SPIE · 0277-786X/02/$15.00

2. CRYSTAL GROWTH

Series of 11 samples of $LiY_{1-x}Er_xF_4$ crystals with the dopant concentration 0.3 – 100 at. % were studied. Crystals $LiY_{1-x}Er_xF_4$ (x=0.003-1) were grown by the modified Stockbarger-Bridgmen technique from a mixture with stoichiometric composition prepared by a hard-phase method. Crystals were grown from graphite crucibles in high vacuum. Single crystals of high optical quality were 8 mm in diameter and 40-50 mm long. Samples for spectroscopic studies with dimensions 5x6x6 mm^3 were parallelepipeds with polished faces and optical axis "c" directed along a rib.

3. EXPERIMENTAL METHODS

Experimental measurements were performed with steady-state and kinetic emission spectroscopy. Relative changes in the steady-state population of studied levels were experimentally controlled by luminescence spectra of the crystals in the wavelength range of radiative transitions $^4S_{3/2} \rightarrow {}^4I_{15/2}$ (0.52 - 0.57) μm and $^4F_{9/2} \rightarrow {}^4I_{15/2}$ (0.64 - 0.68) μm. Spectra were recorded with a computer-controlled photoelectric set-up based on an MDR-23 monochromator. Erbium ions were excited into $^4I_{11/2}$ level (transition $^4I_{15/2} \rightarrow {}^4I_{11/2}$). Selective excitation of $^4I_{11/2}$ level was produced by emission of InGaAs laser diodes. For this purpose we used either a DL-5M module (λ = 964 - 981 nm, 5W, fiber output with a 230 μm in diameter) or a single laser diode (λ = 972 nm, 1W). The single diode face area was transferred directly to the sample by focusing system.

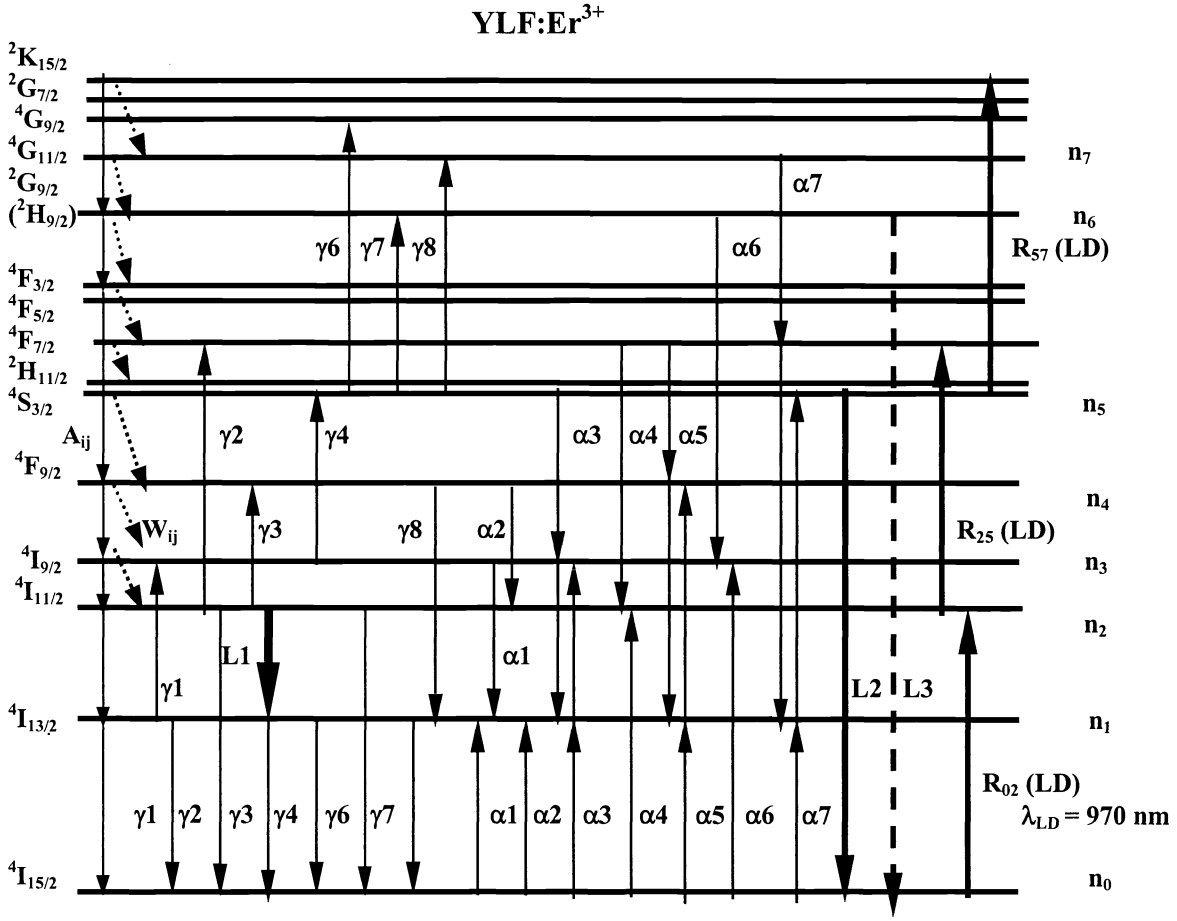

Figure 1. Energy levels and schemes of non-radiative Er-Er coupling in YLF:Er^{3+}. Thin arrows – non-radiative energy transfer: γ – upconversion, α – selfquenching, A_{ji} – radiative transitions, and W_{ji} (short dashed arrows) – multiphonon relaxation. Bold arrows: R_{ij} – LD pumping, laser transitions: L1 – 2.8 μm, L2 – 550 nm, and L3 – promising 410 nm.

The luminescence decay curves of Er^{3+} doped crystals were studied under selective laser excitation by a Q-switch Yb-Er–glass laser operating at 1.5 μm (E_{out} ~ 7 mJ, T_{pulse} ~ 20 ns, variable repetition rate). Laser emission was focused on the sample, the luminescence kinetics at different pumping power densities was detected at the wavelengths emitted from $^4S_{3/2}$ and $^2H_{9/2}$ excited Er^{3+} levels, transitions $^4S_{3/2} \rightarrow {}^4I_{15/2}$ and $^2H_{9/2} \rightarrow {}^4I_{15/2}$, respectively. The sample luminescence was analyzed with a monochromator and detected with a photo-multiplayer tube. This experimental set-up was computer-controlled. The decay times were measured using a digital C9-8 oscilloscope. The dynamic range of detection exceeded two orders of magnitude.

Computer simulations were carried out for the spectroscopic model involving 7 lower radiative excited states of erbium ions (n_1, $n_2 \ldots n_7$ in Fig. 1) taking into account the multi-ion interaction in the whole system. System of rate equations for populations of the excited levels of erbium ions was solved and the population dependencies on the dopant concentration and pump power density were derived. The rates of all principal processes of intra- and inter-center coupling were determined from the independent experimental results and theoretical estimations within the framework of known energy transfer theory.

4. RESULTS AND DISCUSSION

Theoretical steady-state populations of erbium levels under different pumping power densities were obtained from the rate balance equations for 8 lowest erbium levels involving intracenter relaxation and inter-ionic coupling processes such as luminescence selfquenching and upconversion. All processes involved into calculations under IR LD excitation of YLF: Er^{3+} crystals, are shown in the energy-level diagram (Fig. 1).

The following system of rate balance equations for normalized level populations was considered:

$$n_0 + n_1 + n_2 + n_3 + n_4 + n_5 + n_6 + n_7 = 1$$

$$dn_1/dt = -A_{10}n_1 + \sum_{i=2}^{7} A_{i1}n_i + 2\alpha_1 n_0 n_3 + \alpha_2 n_0 n_4 + \alpha_3 n_0 n_5 - 2\gamma_1 (n_1)^2 - \gamma_3 n_1 n_2 - \gamma_4 n_1 n_3 - \gamma_7 n_1 n_5 + \gamma_8 n_4 n_5 = 0$$

$$dn_2/dt = -\sum_{j=0}^{1} A_{2j}n_2 + \sum_{i=3}^{7} A_{i2}n_i + W_{32}n_3 + \alpha_2 n_0 n_4 + 2\alpha_4 n_0 n_5 - 2\gamma_2 (n_2)^2 - \gamma_3 n_1 n_2 - \gamma_6 n_2 n_5 + R_{02}n_0 - R_{25}n_2 = 0$$

$$dn_3/dt = -\sum_{j=0}^{2} A_{3j}n_3 - W_{32}n_3 + \sum_{i=4}^{7} A_{i3}n_i + W_{43}n_4 - \alpha_1 n_0 n_3 + \alpha_3 n_0 n_5 + \gamma_1 (n_1)^2 - \gamma_4 n_1 n_3 = 0$$

$$dn_4/dt = -\sum_{j=0}^{3} A_{4j}n_4 + (A_{54} + W_{54})n_5 + A_{64}n_6 + A_{74}n_7 - W_{43}n_4 - \alpha_2 n_0 n_4 + \gamma_3 n_1 n_2 - \gamma_8 n_4 n_5 = 0$$

$$dn_5/dt = -\sum_{j=0}^{4} A_{5j}n_5 + (W_{65} + A_{65})n_6 + A_{75}n_7 - (R_{57} + W_{54})n_5 - (\alpha_3 + \alpha_4)n_0 n_5 + \gamma_2 (n_2)^2 + \gamma_4 n_1 n_3 - (\gamma_7 n_1 + \gamma_8 n_4 + \gamma_6 n_2)n_5 + R_{25}n_2 = 0$$

$$dn_6/dt = -\sum_{j=0}^{5} A_{6j}n_6 + A_{76}n_7 + W_{76}n_7 - W_{65}n_6 + \gamma_7 n_1 n_5 = 0$$

$$dn_7/dt = -\sum_{j=0}^{6} A_{7j}n_7 - W_{76}n_7 + \gamma_6 n_2 n_5 + \gamma_8 n_4 n_5 + R_{57}n_5 = 0$$

Here, $n(\mathrm{Er}) = \Sigma n_i(\mathrm{Er}) = N_{Er}/xN_Y = 1$, where N_Y is the number of yttrium sites per unit volume substituted for erbium, N_{Er} is the concentration of Er^{3+} ions in crystals, x is the relative erbium concentration. In other words, the concentration of Er ions on the i-th excited level is $N_i = n_i x N_Y$ and $\Sigma_i N_i = xN_Y \Sigma_i n_i = N_{Er}$ is the erbium concentration in given sample. The coefficients A_{ij} [s^{-1}] are the probabilities of the radiative transitions from the "i" to "j"levels; (calculated with intensity parameters Ω_t: $\Omega_2 = 1.88 \cdot 10^{-20}$; $\Omega_4 = 0.55 \cdot 10^{-20}$ and $\Omega_6 = 1.56 \cdot 10^{-20} \mathrm{cm}^2$), W_{ij}[s^{-1}] are the probabilities of non-radiative transitions, parameters α_i (i = 1--7) and γ_j (j = 1--8) are the rates of the non-radiative energy transfer in case of selfquenching (α_i) and upconversion (γ_j) via cross-relaxation schemes upon Er – Er coupling (Fig. 1). Parameters of radiative and non-radiative relaxation for YLF:Er^{3+} (x=0.003-1), and the measured values of A_{ij}, W_{ij}, and excited level lifetimes in low-concentrated samples (x = 0.3%) are given in the Table 1.

Table 1. Experimental and calculated transition probabilities for radiative (A_{ij}, s^{-1}) and non-radiative (W_{ij}, s^{-1}) energy-relaxation processes in YLF-Er^{3+}.

$(i \rightarrow j)$	A_{ij}, s^{-1}	W_{ij}, $(\tau_{exp})^{-1}$, s^{-1}	$(I \rightarrow j)$	A_{ij}, s^{-1}	W_{ij}, $(\tau_{exp})^{-1}$, s^{-1}
$^4I_{13/2} \rightarrow {}^4I_{15/2}$	$A_{10} = 91$	$W_{10}=0$, (90)	$^2G_{9/2}(^2H_{9/2}) \rightarrow {}^4I_{15/2}$	$A_{60} = 1037$	$(7.7 \cdot 10^4)$
$^4I_{11/2} \rightarrow {}^4I_{15/2}$	$A_{20} = 115$	(250)	$^2G_{9/2}(^2H_{9/2}) \rightarrow {}^4I_{13/2}$	$A_{61} = 860$	
$^4I_{11/2} \rightarrow {}^4I_{13/2}$	$A_{21} = 15$	$W_{21}=0$	$^2G_{9/2}(^2H_{9/2}) \rightarrow {}^4I_{11/2}$	$A_{62} = 170$	
$^4I_{9/.2} \rightarrow {}^4I_{15/2}$	$A_{30} = 42$	$(1.4 \cdot 10^5)$	$^2G_{9/2}(^2H_{9/2}) \rightarrow {}^4I_{9/2}$	$A_{63} = 12$	
$^4I_{9/.2} \rightarrow {}^4I_{13/2}$	$A_{31} = 45$		$^2G_{9/2}(^2H_{9/2}) \rightarrow {}^4F_{9/2}$	$A_{64} = 12$	
$^4I_{9/.2} \rightarrow {}^4I_{11/2}$	$A_{32} = 0.5$	$W_{32} = 69$	$^2G_{9/2}(^2H_{9/2}) \rightarrow {}^4S_{3/2}$	$A_{6....5} = 10$	$W_{65}= 30$
$^4F_{9/2} \rightarrow {}^4I_{15/2}$	$A_{40} = 717$	$(3 \cdot 10^4)$	$^2G_{9/2} \rightarrow {}^2H_{11/2}$	$A_{6.5'} = 7$	
$^4F_{9/2} \rightarrow {}^4I_{13/2}$	$A_{41} = 29$		$^4G_{11/2} \rightarrow {}^4I_{15/2}$	$A_{70} = 6671$	$(\sim 10^8)$
$^4F_{9/2} \rightarrow {}^4I_{11/2}$	$A_{42} = 57$		$^4G_{11/2} \rightarrow {}^4I_{13/2}$	$A_{71} = 958$	
$^4F_{9/2} \rightarrow {}^4I_{9/2}$	$A_{43} = 1.4$	$W_{43}= 32$	$^4G_{11/2} \rightarrow {}^4I_{11/2}$	$A_{72} = 34$	
$^4S_{3/2} \rightarrow {}^4I_{15/2}$	$A_{50} = 1062$	$(2.5 \cdot 10^3)$	$^4G_{11/2} \rightarrow {}^4I_{9/2}$	$A_{73} = 78$	
$^4S_{3/2} \rightarrow {}^4I_{13/2}$	$A_{51} = 450$		$^4G_{11/2} \rightarrow {}^4F_{9/2}$	$A_{74} = 186$	
$^4S_{3/2} \rightarrow {}^4I_{11/2}$	$A_{52} = 33$		$^4G_{11/2} \rightarrow {}^4S_{3/2}$	$A_{7...5} = 30$	$W_{76}= 200$
$^4S_{3/2} \rightarrow {}^4I_{9/2}$	$A_{53} = 48$		$^4G_{11/2} \rightarrow {}^2H_{11/2}$	$A_{75'} = 10$	
$^4S_{3/2} \rightarrow {}^4F_{9/2}$	$A_{54} = 1$	$W_{54}= 2.2$	$^4G_{11/2} \rightarrow {}^2G_{9/2}(^2H_{9/2})$	$A_{76} = 1$	

Table 2. Schemes of Er^{3+} - Er^3 coupling and the appropriate calculated microparameters of migration (C_{DD}) at multipole-multipole (*mm*) interactions in YLF-Er^{3+} crystals (*dd* – dipole-dipole, *dq* – dipole-quadrupole, and *qq* – quadrupole-quadrupole couplings).

Level	Cross-relaxation transition $(j \rightarrow i)_a$: $(i \rightarrow j)_b$	$C_{DD}^{dd} \cdot 10^{40}$ $cm^6 s^{-1}$	$C_{DD}^{dq} \cdot 10^{55}$ $cm^8 s^{-1}$	$C_{DD}^{qq} \cdot 10^{70}$ $cm^{10} s^{-1}$
1. $^4I_{13/2}$	$(^4I_{13/2} \rightarrow {}^4I_{15/2})$:$(^4I_{15/2} \rightarrow {}^4I_{13/2})$	24.43	21.04	33.77
2. $^4I_{11/2}$	$(^4I_{11/2} \rightarrow {}^4I_{15/2})$:$(^4I_{15/2} \rightarrow {}^4I_{11/2})$	1.557	8.54	87.25
3. $^4I_{9/2}$	$(^4I_{9/.2} \rightarrow {}^4I_{15/2})$:$(^4I_{15/2} \rightarrow {}^4I_{9/2})$	0.167	0	0
4. $^4F_{9/2}$	$(^4F_{9/2} \rightarrow {}^4I_{15/2})$:$(^4I_{15/2} \rightarrow {}^4F_{9/2})$	4.67	0	0
5. $^4S_{3/2}$	$(^4S_{3/2} \rightarrow {}^4I_{15/2})$:$(^4I_{15/2} \rightarrow {}^4S_{3/2})$	1.013	0	0
6. $^2H_{11/2}$	$(^2H_{11/2} \rightarrow {}^4I_{15/2})$:$(^4I_{15/2} \rightarrow {}^2H_{11/2})$	8.7	599	64750
7. $^4F_{7/2}$	$(^4F_{7/2} \rightarrow {}^4I_{15/2})$:$(^4I_{15/2} \rightarrow {}^4F_{7/2})$	6.16	0	0
8. $^2G_{9/2}(^2H_{9/2})$	$(^2G_{9/2} \rightarrow {}^4I_{15/2})$:$(^4I_{15/2} \rightarrow {}^2G_{9/2})$	0.88	0	0
9. $^4G_{11/2}$	$(^4G_{11/2} \rightarrow {}^4I_{15/2})$:$(^4I_{15/2} \rightarrow {}^4G_{11/2})$	13.86	527	10^5

Table 3. Schemes of Er^{3+} - Er^3 coupling and the appropriate calculated microparameters of selfquenching and upconversion (C_{DA}) at multipole-multipole (*mm*) interactions in YLF-Er^{3+} crystals (*dd* – dipole-dipole, *dq* – dipole-quadrupole, and *qq* – quadrupole-quadrupole couplings).

Process	Transition $(j\rightarrow i)_a$:$(j\rightarrow i)_b$ via cross-relaxation scheme	$C_{DA}^{dd}\cdot 10^{40}$, cm^6s^{-1}	$C_{DA}^{dq}\cdot 10^{55}$, cm^8s^{-1}	$C_{DA}^{qq}\cdot 10^{70}$, $cm^{10}s^{-1}$
	Er-Er selfquenching			
α_1	1. $(^4I_{9/2}\rightarrow {}^4I_{13/2})$:$(^4I_{15/2}\rightarrow {}^4I_{13/2})$ - hω	0.60	0.54	0.05
α_2	2. $(^4F_{9/2}\rightarrow {}^4I_{11/2,13.2})$:$(^4I_{15/2}\rightarrow {}^4I_{13/2,11.2})$ - 2hω	0.02	0.094	0.12
α_3	3. $(^4S_{3/2}\rightarrow {}^4I_{9/2,\ 13/2})$:$(^4I_{15/2}\rightarrow {}^4I_{13/2,\ 9/2})$ - hω	12	9.68	0
α_4	4. $(^4F_{7/2}\rightarrow {}^4I_{11/2})$:$(^4I_{15/2}\rightarrow {}^4I_{11/2})$	4.87	33.07	64.91
α_5	5. $(^4F_{7/2}\rightarrow {}^4F_{9/2}, {}^4I_{13/2})$:$(^4I_{15/2}\rightarrow {}^4I_{13/2}, {}^4F_{9/2})$	4.97	118.4	185.5
α_6	6. $(^2G_{9/2}\rightarrow {}^4S_{3/2}, {}^4I_{13/2})$:$(^4I_{15/2}\rightarrow {}^4I_{13/2}, {}^4S_{3/2})$	3.1	38.7	0
	7. $(^2G_{9/2}\rightarrow {}^4I_{9/2})$:$(^4I_{15/2}\rightarrow {}^4I_{9/2})$	0.12	6.8	0
α_7	8. $(^4G_{11/2}\rightarrow {}^4F_{7/2}, {}^4I_{13/2})$:$(^4I_{15/2}\rightarrow {}^4I_{13/2}, {}^4F_{7/2})$-hω	1.54	64	89.3
	Er-Er upconversion			
γ_1	1. $(^4I_{13/2}\rightarrow {}^4I_{9/2})$:$(^4I_{13/2}\rightarrow {}^4I_{15/2})$ + hω	47	42.2	2.76
γ_2	2. $(^4I_{11/2}\rightarrow {}^4F_{7/2})$:$(^4I_{11/2}\rightarrow {}^4I_{15/2})$	4.15	30.36	60.3
γ_3	3. $(^4I_{11/2}\rightarrow {}^4F_{9/2})$:$(^4I_{13/2}\rightarrow {}^4I_{15/2})$ + 2hω	1.4	7.2	9.7
	4. $(^4I_{13/2}\rightarrow {}^4F_{9/2})$:$(^4I_{11/2}\rightarrow {}^4I_{15/2})$ + 2hω	0.027	2.6	2.1
γ_4	5. $(^4I_{9/2}\rightarrow {}^4S_{3/2})$:$(^4I_{13/2}\rightarrow {}^4I_{15/2})$ + hω	27.6	23.77	0
	6. $(^4I_{13/2}\rightarrow {}^4S_{3/2})$:$(^4I_{9/2}\rightarrow {}^4I_{15/2})$ + hω	2.1	0	0
γ_5	7. $(^4F_{9/2}\rightarrow {}^4F_{7/2})$:$(^4I_{13/2}\rightarrow {}^4I_{15/2})$ + 2hω	0.15	2.6	3.2
γ_6	11. $(^4S_{3/2}, {}^4I_{11/2}\rightarrow {}^4G_{11/2})$:$(^4I_{11/2}, {}^4S_{3/2}\rightarrow {}^4I_{15/2})$ + 2hω	10.5	13.5	0
γ_7	9. $(^4I_{13/2}, {}^4S_{3/2}\rightarrow {}^2G_{9/2})$:$(^4S_{3/2}, {}^4I_{13/2}\rightarrow {}^4I_{15/2})$	18.1	117	0
γ_8	10. $(^4S_{3/2}, {}^4F_{9/2}\rightarrow {}^4G_{11/2})$:$(^4F_{9/2}, {}^4S_{3/2}\rightarrow {}^4I_{13/2})$	37.4	801	0

Rates of selfquenching and upconversion were obtained in the analytical form from the theoretically calculated transfer microparameters. Microparameters for all the processes of energy transfer under multipole-multipole (*mm*) coupling involved into calculations are listed in Tables 2 and 3. From the analysis of the data obtained we chose the dominant energy transfer mechanism for each particular scheme, and the formulae connecting the transfer microparameters with the macrorates of selfquenching and upconversion processes for the jumping and static ordered decay models.

For the processes of selfquenching, the transfer microparameters depend on erbium concentration and population of the ground state $N_0 \equiv n_0(\mathrm{Er})N_{Er}$. For the upconversion processes, the rate of non-linear coupling is connected with the population of the excited states. Otherwise, population of the ground and excited states could be

expressed as a product of dopant concentration and normalized population n_i of the *i* level, i. e. via the arguments of the system of equations. Therefore, concentration dependencies of the parameters α and γ could be written in the analytical form. Disregarding the case of high pump-power densities, the normalized population of the ground state was set close to 1, in other words, the dopant concentration was employed in the formulae of selfquenching.

Analytical form of the calculated macrorates of selfquenching (α_i) and upconversion (γ_j) used in the system of balance equations for $LiY_{1-x}Er_xF_4$ ($x = 0.01 \div 1$ at. %) are given in Table 4. It should be noted that, unlike data reported in other works[5], our theoretical model does not involve any fitting parameters; all magnitudes were obtained from calculated and experimental data.

Table 4. Analytical concentration dependencies of selfquenching (α_i) and upconversion parameters (γ_i) in $LiY_{1-x}Er_xF_4$. Parameters were calculated in jumping (JM) and static-decay (SM) models with calculated transfer microparameters C_{DA} and C_{DD}, $x = N_{Er}/N_Y$ –relative erbium concentration, n_i (i = 0, 1....7) - relative populations of erbium levels.

Model, Transition $(j \rightarrow i)_a$: $(i \rightarrow j)_b$	Parameter, s^{-1}
S. $(^4I_{9/2} \rightarrow {}^4I_{15/2})$:$(^4I_{15/2} \rightarrow {}^4I_{13/2})$ -hω	$\alpha_1 = 1.29\cdot10^5 x^2 + 3.35\cdot10^5\cdot x^{8/3} + 2.85\cdot10^5\cdot x^{10/3}$
J. $(^4F_{9/2} \rightarrow {}^4I_{11/2})$:$(^4I_{15/2} \rightarrow {}^4I_{13/2})$ -2hω	$\alpha_2 = 1.91\cdot10^5 x^2$
S. $(^4S_{3/2} \rightarrow {}^4I_{9/2,\ 13/2})$:$(^4I_{15/2} \rightarrow {}^4I_{13/2,9/2})$-hω	$\alpha_3 = 2.5\cdot10^6 x^2 + 5.96\cdot10^5\cdot x^{8/3}$
J. $(^2H_{11/2} \rightarrow {}^4I_{9/2})$:$(^4I_{15/2} \rightarrow {}^4I_{13/2})$	$\alpha_4 = 5.4\cdot10^6 x^2$
J. $(^4I_{13/2} \rightarrow {}^4I_{9/2})$:$(^4I_{13/2} \rightarrow {}^4I_{15/2})$ +hω	$\gamma_1 = 2.26\cdot10^7 (n_1(0)\cdot x)^2$
S. $(^4I_{11/2} \rightarrow {}^4F_{7/2})$:$(^4I_{11/2} \rightarrow {}^4I_{15/2})$	$\gamma_2 = 8.9\cdot10^5 (n_2(0)\cdot x)^2 + 1.86\cdot10^6 (n_2(0)\cdot x)^{8/3} + 1.16\cdot10^6 (n_2(0)\cdot x)^{10/3}$
J. $(^4I_{11/2} \rightarrow {}^4F_{9/2})$:$(^4I_{13/2} \rightarrow {}^4I_{15/2})$ +2hω	$\gamma_3 = 1.0\cdot10^6 (n_1(0)\cdot x)\ (n_2(0)\cdot x)$
J. $(^4I_{9/2} \rightarrow {}^4S_{3/2})$:$(^4I_{13/2} \rightarrow {}^4I_{15/2})$ + hω	$\gamma_4 = 3.85\cdot10^6 (n_1(0)\cdot x)\ (n_3(0)\cdot x)$
S. $(^4I_{11/2} \rightarrow {}^4I_{15/2})$:$(^4S_{3/2} \rightarrow {}^4G_{11/2})$ + hω	$\gamma_6 = 4.05\cdot10^6 (n_2(0)\ n_5(0))\cdot x^2 + 6.3\cdot10^7 (n_2(0)\cdot n_5(0))^{4/3} x^{8/3} + 9.4\cdot10^7 (n_2(0)\cdot n_5(0))^{5/3} x^{10/3}$
S. $(^4I_{13/2} \rightarrow {}^4I_{15/2})$:$(^4S_{3/2} \rightarrow {}^2G_{9/2}/{}^2H_{9/2})$ - hω	$\gamma_7 = 4.0\cdot10^6 (n_1(0)\ n_5(0))\cdot x^2 + 6.5\cdot10^6 (n_1(0)\cdot n_5(0))^{4/3} x^{8/3}$
S. $(^4F_{9/2} \rightarrow {}^4I_{13/2})$:$(^4S_{3/2} \rightarrow {}^4G_{11/2})$ + hω	$\gamma_8 = 6.0\cdot10^6 (n_4(0)\ n_5(0))\cdot x^2 + 2\cdot10^8 (n_4(0)\cdot n_5(0))^{4/3} x^{8/3}$

In this work we compared the calculated and experimental intensities of the luminescence signal. To do this we had to integrate the value $N_i = n_i \cdot x N_Y$ over excited volume, here $x = N_{Er}/N_Y$ is the relative concentration of erbium ions, $N_Y = 1.39\cdot10^{22}$ cm^{-3} is the number of yttrium sites substituted for erbium per unit volume. To obtain the analytical form of concentration dependence of the parameters of non-linear coupling, one should estimate initial population of the excited levels $N_i(P)$ produced by absorption of pumping radiation P. Let us denote $N_i(P) = n_i(0) x N_Y$. In YLF: Er^{3+} crystals with high erbium concentration, the luminescence intensity in the direction of the pumping beam strongly depends on the distance from the crystal surface because of a strong absorption of pumping radiation in the sample. Spatial dependence of the pump intensity could be expressed with the Bouguer law. However, spatial dependence of the normalized population of the *i* level resulted from the absorption of the pumping quantum $n_i(0)$ cannot be written in the explicit form. Therefore, numerical integrating over the excited volume was carried out for the fixed relative erbium concentrations $x = 0.005 \div 1$. Excited volume of the crystal was divided into separate layers. For a individual layer separated by the distance r from the sample surface, the pump power density $P(r)$ was determined with the Bouguer law $P(r) = P_0 \exp(-\Sigma\sigma_{ij}\ n_i(0) x N_Y\ r)$, where P_0 is the pump power density. $R_{ij} = \sigma_{ij} P/p_0$ are the rates of absorption transitions for the quantum energy of pumping photons $p_0 = hc/\lambda_p$. For calculations we used the values of the ground state absorption (GSA) for R_{02} ($\lambda_{LD1=\ 972nm}$) = $0.6\cdot10^{-20}$ ($^4I_{15/2} \rightarrow {}^4I_{11/2}$ transition); excited state absorption (ESA) for R_{25}

($\lambda_{LD\,=\,968nm}$) = (0.5-1)·10^{-20} ($^4I_{11/2} \rightarrow {}^4F_{7/2}$), and for R_{57} ($\lambda_{LD\,=\,970\ nm}$) = 0.51·10^{-20} ($^4S_{3/2} \rightarrow {}^2G_{7/2},{}^2K_{15/2}$). Reabsorption at laser wavelength was not taken into account. The system of rate balance equations was solved for pumping with one type of laser diode LD1 (968-972 nm). The results are compared with experimental concentration and power dependences of luminescence intensity from $^4S_{3/2}$ (at 550 nm) and $^4F_{9/2}$ (at 650 nm) levels, the dependences of luminescence intensity from $^2G_{9/2}(^2H_{9/2})$ and from $^4G_{11/2}$ levels are considered only theoretically. Concentration dependences of populations were calculated for the same pump-power densities, which were used in the experiments. Power dependencies were calculated for erbium concentrations varied from 1 to 30%. Corresponding calculated dependences are shown in Figs. 2 - 5.

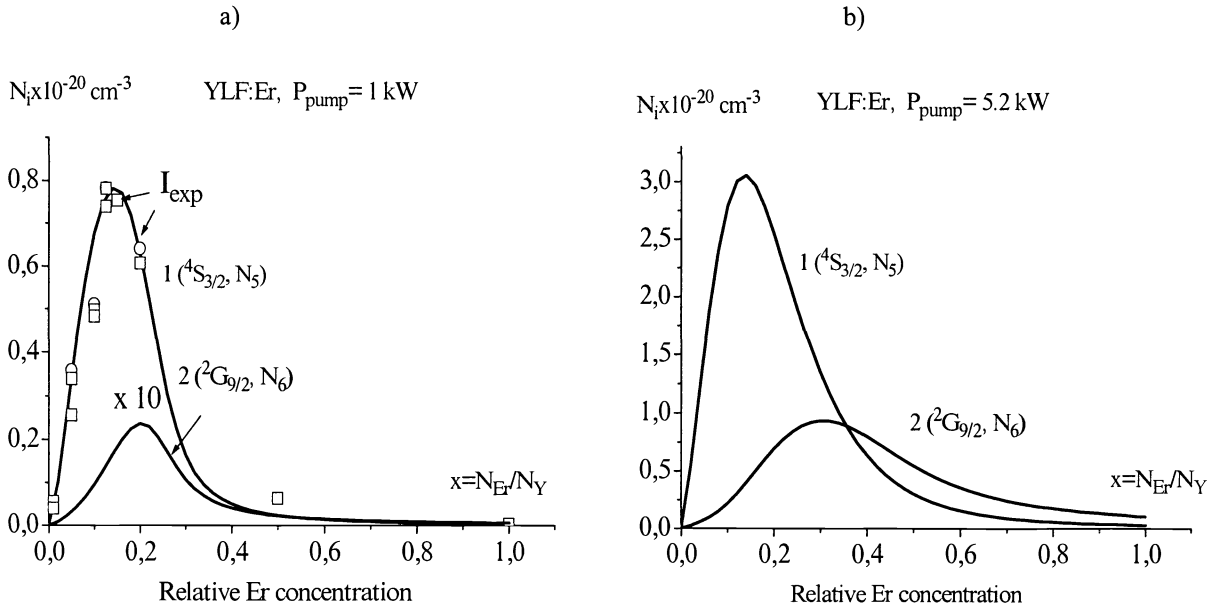

Figure 2. Calculated and experimental (squares) concentration dependences of steady-state population N_i of excited "green" laser $^4S_{3/2}$ (curves 1) and " blue" $^2G_{9/2}$ ($^2H_{9/2}$) (curves 2) levels under cw pumping with a single InGaAs laser diode. a) - pump power density 5.2 kW/cm^2. Values for "blue" level are multiplied by 10. b) - pump power density 26 kW/cm^2. T = 300^0 K.

Experimental concentration and power dependences of populations of $^4S_{3/2}$ (N_5) and $^4F_{9/2}$ (N_4) erbium levels in YLF:Er^{3+} crystals with x=0.003 ÷ 1 were obtained from the luminescence spectra recorded at pump power density up to 5.2 kW/cm^2. Comparison of the calculated and experimental results is shown in Figs. 2 - 5. A sample of the upconversion luminescent spectrum of YLF:Er^{3+} (1 at. %, x=0.01) crystal is given on Fig. 6.

As follows from Figs 2, 3 population of $^4S_{3/2}$ and $^4F_{9/2}$ levels at pump power density about 5 kWcm^{-3} increases with erbium concentration up to the maximum in the region $N_{Er} \approx 10 \div 15$ at% and decreases in the range of $N_{Er} > 15$ at%. Luminescence from $^4G_{11/2}$ level is considerably quenched. The population of $^2G_{9/2}$ ($^2H_{9/2}$) level increases with growing of Er concentration and pump power density (Figs. 2) due to increasing of upconversion rates. Behavior of the population of $^2G_{9/2}$ ($^2H_{9/2}$) level for low pump power densities is similar to that of green level. This agrees with results of kinetic measurements (Fig. 7) showing decay curves of green and blue luminescence upon pulsed IR laser pumping.

Experimental dependences of population of the $^4S_{3/2}$ and $^4F_{9/2}$ levels on the pump power density were measured in all 11 samples for pump power densities 730, 2470, 3360, and 5200 W/cm^2. As follows from Figs. 2 and calculated power dependencies of populations of the ground $^4I_{15/2}$ and excited $^4S_{3/2}$ and $^2G_{9/2}$ ($^2H_{9/2}$) states (Fig. 5), erbium concentration for green lasing in YLF:Er^{3+} on the $^4S_{3/2} \rightarrow {}^4I_{15/2}$ transition under CW pumping of $^4I_{11/2}$ level should not exceed 10 – 15 at. % and pump power density should be higher 6 kW/cm^2. The population of the $^2G_{9/2}$ ($^2H_{9/2}$) level increases considerably at pump power density more than 5 kWcm^{-3} (Fig. 4), but the blue lasing on the $^2G_{9/2}$ ($^2H_{9/2}$) $\rightarrow {}^4I_{15/2}$ transition cannot be achieved at room temperature in the range of pump-power densities available from the contemporary cw IR laser diodes.

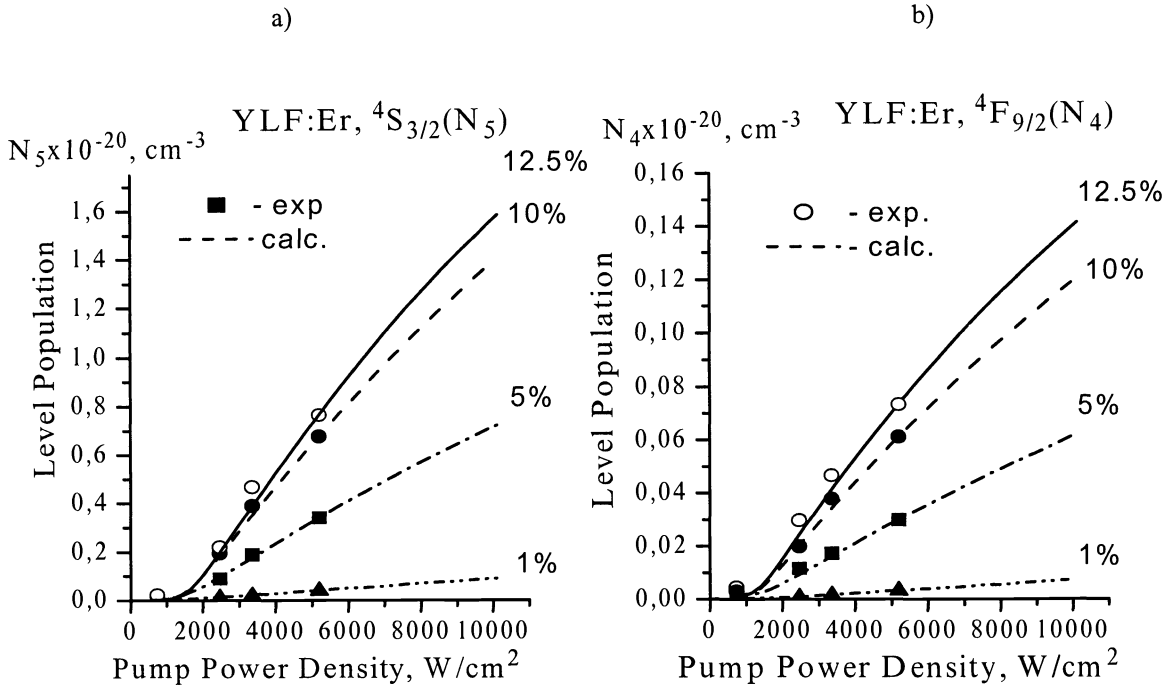

Figure 3. Calculated (curves) and experimental (symbols) dependences of steady-state populations $N_i(P_{pump})$ of excited $^4S_{3/2}$ (a) and $^4F_{9/2}$ (b) levels on pump power density $N_i = f(P_{pump})$ under cw pumping with a single InGaAs laser diode in YLF:Er^{3+} crystals with different Er concentrations: 1, 5, 10 and 12.5 at. %. T = 300^0 K. a) populations $N_5(P_{pump})$ of $^4S_{3/2}$ level in YLF:Er^{3+} crystals with Er concentrations: 1, 5, 10 and 12.5 at. %. b) populations $N_4(P_{pump})$ of $^4F_{9/2}$ level in YLF:Er^{3+} crystals with Er concentrations: 1, 5, 10 and 12.5 at. %.

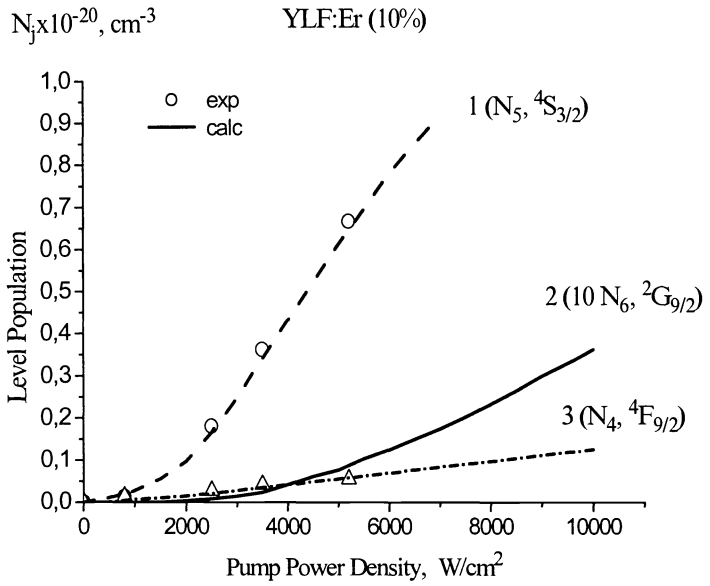

Figure 4. . Calculated (curves) and experimental (symbols) power dependences of populations N_i of excited states in YLF:Er^{3+} crystal (10 at. %, x=0.1) under pumping with laser diodes: $^4F_{9/2}$ (N_4) – open triangles (curve 3), $^4S_{3/2}$ (N_5) – open circles (curve 1); $^2G_{9/2}(^2H_{9/2})$ (N_6) – theory only (curve 2). Values, which represent population of $^2G_{9/2}(^2H_{9/2})$ state, are multiplied by factor of 10. T = 300^0 K.

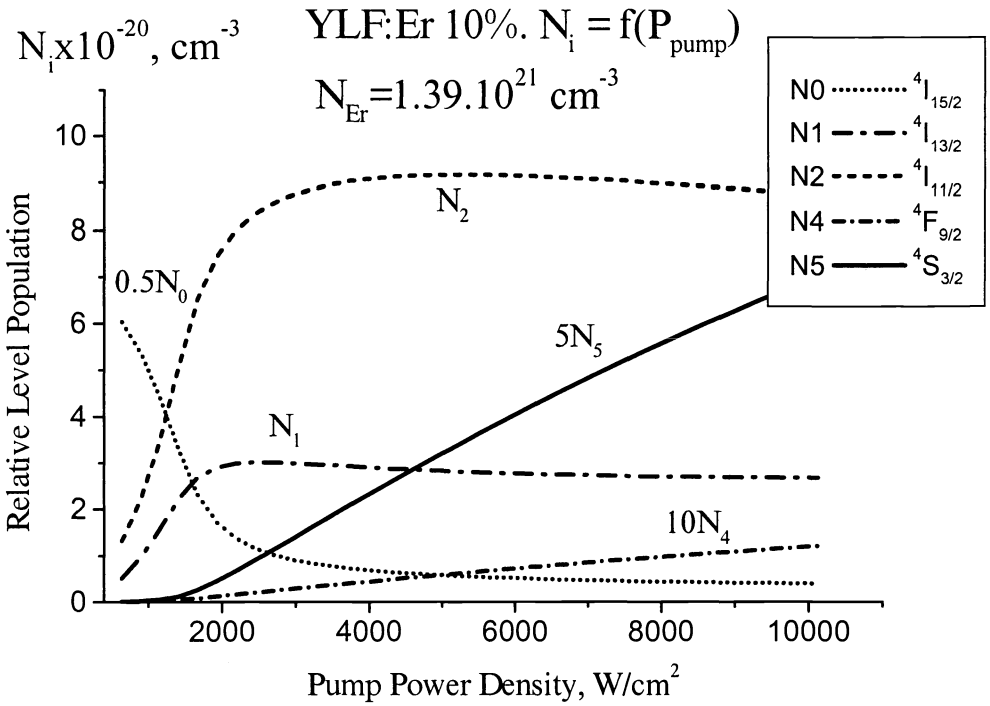

Figure 5. Calculated dependences of steady-state populations $N_i = n_i x N_Y$ of ground and lower excited states of Er ions on pump-power density under cw pumping with a single InGaAs laser diode in YLF:Er^{3+} (10 at. %) crystal. T=300^0 K.

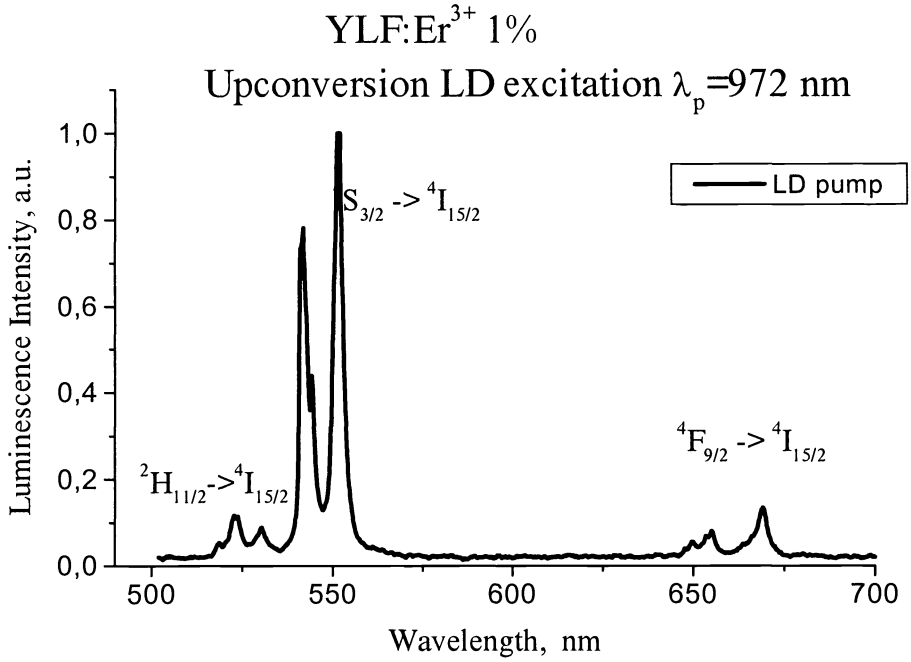

Figure 6. Upconversion luminescent spectrum of YLF:Er^{3+} (1 at. %, x=0.01) crystal. Excitation with a single InGaAs laser diode. Transitions from $^2H_{11/2}$, $^4S_{3/2}$, and $^4F_{9/2}$ levels. T = 300^0 K.

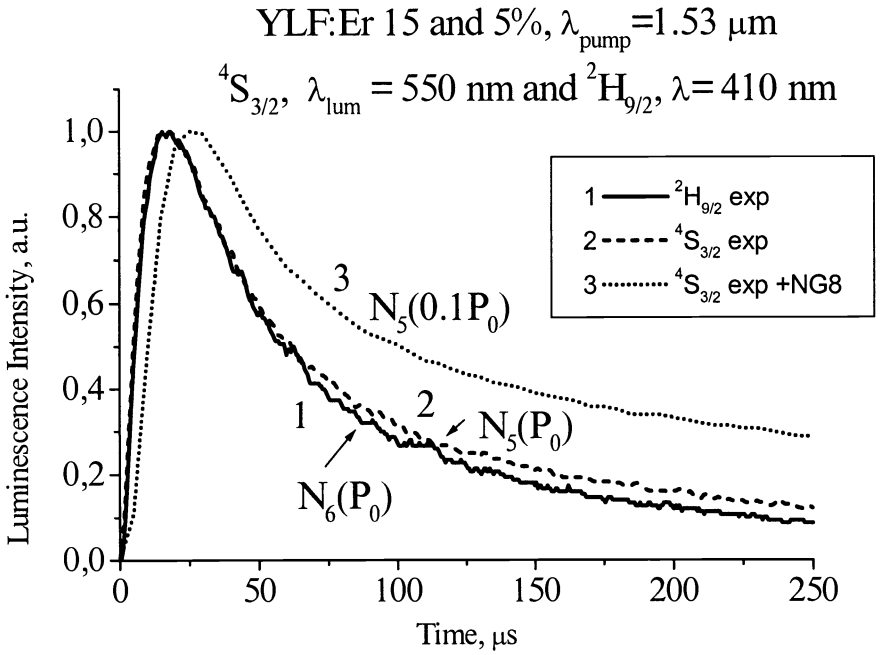

Figure 7. Luminescence decay curves for erbium transitions $^2G_{9/2}$ ($^2H_{9/2}$) → $^4I_{15/2}$ (curve 1, λ_{lum} = 410 nm) and $^4S_{3/2}$ → $^4I_{15/2}$ (curves 2 and 3, luminescence wavelength λ_{lum} = 550 nm) upon selective pulsed laser excitation at λ_{exc} = 1.5 μm. T=300^{0}K.

Calculated theoretical results are in good agreement with represented experimental data. Agreement between theoretical and experimental data obtained in these studies enables assumption on the proper description of the populations of the levels studied in the range of higher pump power densities.

5. CONCLUSION

Similar to previously reported studies, theoretical calculations with the energy transfer constants of selfquenching and upconversion obtained by the method of model quantum-mechanical calculation show good agreement with theoretical results. Therefore, a conclusion could be made that population of erbium excited levels in $LiY_{1-x}Er_xF_4$ (x=0.003 ÷1) can be reliably described with thus-proposed spectroscopic model and the rate balance equations allowing for the non-linear energy transfer processes. The conclusion was made, that green lasing in YLF:Er^{3+} on the $^4S_{3/2}$ → $^4I_{15/2}$ transition under CW pumping of $^4I_{11/2}$ level may be achieved with upconversion pumping with laser diodes emitting at 968-972 nm, but the blue cw lasing on the $^2G_{9/2}$ ($^2H_{9/2}$) → $^4I_{15/2}$ transition cannot be achieved at room temperature in the range of pump-power densities about 6 kW/cm^2 available from the contemporary cw IR laser-diodes. Pulse laser action on the transitions originating from the $^2G_{9/2}$ ($^2H_{9/2}$) and the $^4G_{11/2}$ levels in YLF:Er^{3+} crystals may be realised at room temperature with upconversion pumping by IR short pulse. At low temperature (40^{0}K) upconversion cw laser action at 560.6 nm (transition $^2H_{9/2}$ → $^4I_{13/2}$) was observed in under IR pumping by Ti-sapphire laser.[6]

ACKNOWLEDGMENTS

The work was partly supported by INTAS, Grant No. INTAS-97-787, and Russian Foundation for Basic Researches, Grants No. 00-02-16637.

REFERENCES

1. A.M. Tkachuk., I.K. Razumova, A.A. Mirzaeva, G.E. Novikov, O.A. Orlov, A.V. Malyshev, and V.P. Gapontsev, "Concentration and power dependences of level population of 2.8 - μm laser transition in YLF : Er crystals under CW laser diode pumping". *Proceed. SPIE* **4350** (11), pp.75-80, 2000.

2. A.M. Tkachuk., I.K. Razumova, A.A. Mirzaeva, A.V. Malyshev, and V.P. Gapontsev, "Population of Er^3 levels in $LiY_{1-x}Er_xF_4$ (x=0.003 ÷1) crystals under steady-state pumping by InGaAs laser diodes", *J Opt Technol* **67**, (9), pp. 851-853, 2000.
3. A.M. Tkachuk., I.K. Razumova, A.V. Malyshev, and V.P. Gapontsev, "Population of lasing erbium levels under upconversion cw LD pumping", *J. Lumin.* **00**, (0), 2001, in press.
4. A.M. Tkachuk., I.K. Razumova, A.A. Mirzaeva, A.V. Malyshev, and V.P. Gapontsev, "Upconversion and population of excited erbium levels in $LiY_{1-x}Er_xF_4$ (x =0.003 --1) crystals under CW InGaAs laser-diode pumping", *Opt. Spectrosc.* **92**, (1), pp. 00-00, 2002, in press.
5. M. Tikerpae, S.D. Jackson , and T.A. King, "Theoretical comparison of Er^{3+}-doped crystal lasers", *J. of Modern Optics* **45**, (6), pp. 1269-1284, 1998.
6. T. Hebert, R. Wannemacher, W. Lenth, and R.M. Macfarline, "Blue and green cw upconversion lasing in Er:$YLiF_4$", *Appl. Phys Lett.* **57** (17), pp. 1727-1729, 1990